High Performance Simple Position Neuro-Controller for Field-Oriented Induction Motor Servo Drives

[1] FAYEZ F. M. EL-SOUSY [2] M. M. SALEM
[1-2] Power Electronics @ Energy Conversion Department
[1-2] Electronics Research Institute (ERI)
Al-Tahrir Street, Dokki, Giza, Egypt
EGYPT

Abstract:- In this paper, the position control of a detuned indirect field oriented control (IFOC) induction motor drive is studied. A proposed Simple–Neuro-Controllers (SNCs) are designed and analyzed to achieve high-dynamic performance both in the position command tracking and load regulation characteristics for robotic applications. The proposed SNCs are trained on-line based on the back propagation algorithm with a modified error function. Four SNCs are developed for position, speed and d-q axes stator currents respectively. Also, a synchronous proportional plus integral-derivative (PI-D) two-degree-of-freedom (2DOF) position controller and PI-D speed controller are designed for an ideal IFOC induction motor drive with the desired dynamic response. The performance of the proposed SNCs and synchronous PI-D 2DOF position controllers for detuned field oriented induction motor servo drive is investigated. Simulation results show that the proposed SNCs controllers provide high-performance dynamic characteristics and are robust with regard to motor parameter variations and external load disturbance. Furthermore, comparing with the synchronous PI-D 2DOF controller demonstrates the superiority of the proposed SNCs controllers due to attain a robust performance for IFOC induction motor servo drive system.

Key-Words: Indirect field orientation control (IFOC), 2DOF PI-D, SNC, induction motor drive

1 Introduction

Induction machine servo drive system is considered high-performance when the rotor position, rotor speed and stator currents can be controlled to follow a reference for tracking at all times. A track is a desired time history of the motor current, speed or position. This servo drive system is essential in many applications such as robotics, actuation, numerically controlled machinery and guided manipulation where precise control is required. Previously, dc machines were used in variable speed and position control applications because of the possibility of controlling their flux and torque independently. However, dc machines have many disadvantages. To overcome the dc machines disadvantages, the induction machines can be used because of its simple and rugged structure, easy maintenance and economical operation.

The induction motor can be controlled similar to a dc motor using field oriented control (FOC) strategy [1-2]. However, difficulties are found from modelling uncertainties due to parameter variations, magnetic saturation and load disturbances. To ensure high dynamic performance various control strategies for field oriented induction motor drive have been reported in the literature.

Conventional control schemes with (PI, IP and PID) have gained the widest acceptance in high-performance servo drives. However, the induction machine parameters variation causes a degradation in the dynamic response for disturbance rejection and tracking performance with these control schemes.

To overcome the drawbacks of the conventional controller and to achieve high- dynamic performance, research in artificial intelligent (such as neural network) as a controller has become increasingly prevalent.

A neural network can be a feed forward or a feedback type. A feed forward multi-layer neural network usually consists of input layer, output layer and one or more hidden layers of neurons. It is well known that the neural networks need to be trained and its training is time consuming. High convergence accuracy and high convergence rate are desirable for the training of the neural network. The most popular training algorithm for a multi-layer neural network is the back propagation [3-9].

In this paper, a simple–neuro-controller (SNCs) are designed and analyzed. Four SNCs are used for position, speed, d-q axis stator currents respectively. Each SNC consists of only one weight and one neuron with a linear hard limit activation function.

The SNC is trained on-line based on the back propagation algorithm with a modified error function. In spite of their simple construction, the obtained results show that the SNCs can provide a fast and accurate dynamic response in tracking and disturbance rejection characteristics under parameter variations. At the same time, a reduction of the computation time has been occurred as a result of the simple construction of the four SNCs. The simulation results have demonstrated that robust control performances both in command tracking and load regulation are achieved by the proposed SNCs controllers when detuning occurs and then improve the dynamic behavior compared with the synchronous PI-D 2DOFC position controller.

The results of the simulation confirm the effectiveness of the proposed SNCs controllers and its superiority as compared with the synchronous PI-D 2DOF position controller for IFOC induction machine drive system. Also, the results demonstrate that the proposed SNCs control scheme has robust position response and can rapidly cancel the load disturbance.

2 Induction Machine Model for Position Control

The block schematic of IFOC-based induction machine servo drive with inverter controlled using space vector modulation (SVM) technique is shown in Fig. 1. The Figure shows that three feedback loops in the control system. The inner is the current feedback loop, the middle is the speed feedback loop and the outer is the position feedback loop. Also, the diagram includes a current regulated pulse width modulation (CRPWM) inverter with SVM technique (CRSVMPWM), indirect field orientation controller (IFOC), decoupling controlling, proposed SNCs for d-q stator current controllers, speed controller and position controller. The ideal and detuned modeling of the induction motor and various control blocks are presented in the following section.

2.1 Nominal Parameters Model

The state equation of the nonlinear dynamic d-q model of the induction machine at the synchronous reference frame is expressed as follows [1,2].

2.2 Detuned Parameters Model

For facilitating the analysis and design of the proposed controllers, a model representing the dynamic behavior of a detuned IFOC for induction machine is developed. Since the detuning of IFOC is mainly due to the variations of the rotor time constant, the decoupling between the torque command and flux command is no ideal and thus the torque response becomes oscillatory and sluggish. From equations 1, 2 and 3, we can derive the perturbed model of the induction machine as given by equations (4-6).

$$\frac{d}{dt}\begin{bmatrix} i_{qs}^e \\ i_{ds}^e \\ \lambda_{qr}^e \\ \lambda_{dr}^e \end{bmatrix} = \begin{bmatrix} -k_{ss} & -\omega_e & \frac{k_m}{\tau_r^*} & -k_m\omega_r \\ \omega_e & -k_{ss} & k_m\omega_r & \frac{k_m}{\tau_r^*} \\ \frac{L_m}{\tau_r^*} & 0 & -\frac{1}{\tau_r^*} & -\omega_{sl} \\ 0 & \frac{L_m}{\tau_r^*} & \omega_{sl} & -\frac{1}{\tau_r^*} \end{bmatrix} \begin{bmatrix} i_{qs}^e \\ i_{ds}^e \\ \lambda_{qr}^e \\ \lambda_{dr}^e \end{bmatrix} + \frac{1}{\sigma L_s}\begin{bmatrix} V_{qs}^e \\ V_{ds}^e \\ 0 \\ 0 \end{bmatrix} \quad (1)$$

$$T_e = \frac{3}{2}.\frac{P}{2}.\frac{L_m}{L_r}(\lambda_{dr}^e i_{qs}^e - \lambda_{qr}^e i_{ds}^e) \quad (2)$$

$$T_e = \frac{J}{(P/2)}\frac{d^2}{dt^2}\theta_r + \frac{\beta}{(P/2)}\frac{d}{dt}\theta_r + T_L \quad (3)$$

2.3 IFOC Model (Decoupling Controller)

The IFOC dynamics for the induction machine (torque, slip angular frequency and voltage commands) can be derived from equations (1-2) respectively at $\lambda_{qr}^e = 0$ and $d\lambda_{qr}^e/dt = 0$. The torque equation and slip angular frequency for rotor field orientation are given in equations (7, 8) while the voltage commands (decoupling controller) of the indirect field orientation controller (IFOC) are given in equations (9-12).

$$\frac{d}{dt}\begin{bmatrix} \Delta i_{qs}^e \\ \Delta i_{ds}^e \\ \Delta\lambda_{qr}^e \\ \Delta\lambda_{dr}^e \end{bmatrix} = \begin{bmatrix} -k_{ss} & -\omega_{e\circ} & \frac{k_m}{\tau_r} & -k_m\omega_{r\circ} \\ \omega_{e\circ} & -k_{ss} & k_m\omega_{r\circ} & \frac{k_m}{\tau_r} \\ \frac{L_m}{\tau_r} & 0 & -\frac{1}{\tau_r} & -\omega_{sl\circ} \\ 0 & \frac{L_m}{\tau_r} & \omega_{sl\circ} & -\frac{1}{\tau_r} \end{bmatrix} \begin{bmatrix} \Delta i_{qs}^e \\ \Delta i_{ds}^e \\ \Delta\lambda_{qr}^e \\ \Delta\lambda_{dr}^e \end{bmatrix} + \frac{1}{\sigma L_s}\begin{bmatrix} \Delta V_{qs}^e \\ \Delta V_{ds}^e \\ 0 \\ 0 \end{bmatrix} \quad (4)$$

$$\Delta T_e = K_t\begin{pmatrix} \lambda_{dr\circ}^e \Delta i_{qs}^e - \lambda_{qr\circ}^e \Delta i_{ds}^e \\ -i_{ds\circ}^e \Delta\lambda_{qr}^e + i_{qs\circ}^e \Delta\lambda_{dr}^e \end{pmatrix} \quad (5)$$

$$\Delta T_e = \frac{J}{(P/2)}\frac{d^2}{dt^2}\Delta\theta_r + \frac{\beta}{(P/2)}\frac{d}{dt}\Delta\theta_r + \Delta T_L \quad (6)$$

$$T_e = \frac{3}{2}.\frac{P}{2}.\frac{L_m^2}{L_r} i_{ds}^{e*} i_{qs}^{e*} \quad (7)$$

$$\omega_{sl} = \frac{1}{\tau_r}.\frac{i_{qs}^{e*}}{i_{ds}^{e*}} \quad (8)$$

$$V_{qs}^{e*} - e_{qs}^{e*} = \left(L_s\sigma\frac{d}{dt}i_{qs}^{e*} + R_s i_{qs}^{e*}\right) \quad (9)$$

$$e_{qs}^{e*} = \left(L_s\sigma + L_m^2 / L_r\right)\omega_e .i_{ds}^{e*} \quad (10)$$

$$V_{ds}^{e*} + e_{ds}^{e*} = \left(L_s\sigma \frac{d}{dt} i_{ds}^{e*} + R_s i_{ds}^{e*}\right) \quad (11)$$

$$e_{ds}^{e*} = \left(L_s\sigma + L_m^2 / L_r\right)\omega_e .i_{qs}^{e*} \quad (12)$$

3 Design of the Proposed PI-D 2DOF Controller

In this section, the analysis and design procedures of different conventional controllers are carried out for a comparison purpose. The PI-D and PI-D 2DOF speed and position controllers respectively are designed. The PI current controllers has been designed in [1]. The design depends on the desired response technique.

3.1 PI-D Speed Controller

According to block diagram shown in Fig. 2, the closed loop transfer function at $T_L(s) = 0$ is given by:

$$\frac{\omega_r(s)}{\omega_r^*(s)} = \frac{K(K_p^\omega s + K_i^\omega)}{s^3 + \tau_{2\omega}s^2 + \tau_{1\omega}s + KK_i^\omega} \quad (13)$$

Where,

$\tau_{1\omega} = (1/\tau_{sr}^{'}\tau_m + KK_p^\omega / \tau_{sr}^{'})$, $\tau_{2\omega} = (1/\tau_{sr}^{'} + 1/\tau_m + KK_d^\omega)$

$K = (K_t K_j K_q / \tau_{sr}^{'})$, $K_j = P/2J$, $K_q = \tau_{sr}^{'} / \sigma L_s$

$K_t = \frac{3}{2}.\frac{P}{2}.\frac{L_m^2}{L_r}.i_{ds}^{e*}$, $\tau_m = J/\beta$,

$\tau_{sr}^{'} = \tau_s^{'}\tau_r^{'} /(\tau_r^{'} + \tau_s^{'}(1-\sigma))$,

$(1+\sigma_r) = L_r / L_m$, $(1+\sigma_s) = L_s / L_m$,

$\sigma = (L_s L_r - L_m^2)/L_s L_r$

$k_{ss} = \left(1/\sigma\tau_s + 1 - \sigma/\sigma\tau_r\right)$

$K_m = L_m / \sigma L_s L_r, \tau_s^{'} = \sigma\tau_s, \tau_r^{'} = \sigma\tau_r, \tau_s = L_s/R_s, \tau_r = L_r/R_r\ \tau_r$

: the detuned rotor time constant

τ_r^* : the nominal rotor time constant

ω_{sl} : the slip angular frequency

ω_n : the natural frequency of the speed loop

e_{ds}^{e*}, e_{ds}^{e*} : the back e.m.f of the machine in d-q axes

V_{ds}^{e*}, V_{ds}^{e*} : the voltage commands in d-q axis

Using the third order performance index based on the ITAE robust technique which has the following equation, we can determine the controller parameters as follows.

$$\frac{C(s)}{R(s)} = \frac{\omega_n^3}{s^3 + 1.75\omega_n s^2 + 2.15\omega_n^2 s + \omega_n^3} \quad (14)$$

From equations (13 and 14), we can determine the controller parameters as follows.

$$K_p^\omega = \frac{2.15\omega_n^3\tau_{sr}^{'} - 1/\tau_m}{K\tau_{sr}^{'}} \quad (15)$$

$$K_i^\omega = \frac{\omega_n^3}{K} \quad (16)$$

$$K_d^\omega = \frac{\left(1.75\omega_n - 1/\tau_{sr}^{'} - 1/\tau_m\right)}{K} \quad (17)$$

3.2 PI-D 2DOF Position Controller

3.2.1 Feed-back Controller

The type of feedback controller is proposed as a PI-D controller while the feed forward controller is designed based on the desired closed loop response [2]. According to block diagram shown in Fig. 3, the closed loop transfer function at $T_L(s) = 0$ is given by the following equation.

$$\frac{\theta_r(s)}{\theta_d(s)} = \frac{K_t K_j (K_p^\theta s + K_i^\theta).(K_p^\omega s + K_i^\omega)/\tau_{2\omega}}{s^4 + \tau_{3\theta}s^3 + \tau_{2\theta}s^2 + \tau_{1\theta}s + \hat{K}K_i^\theta} \quad (18)$$

Using the fourth order performance index based on the ITAE robust technique which has the following equation, we can determine the controller parameters as follows.

$$\frac{C(s)}{R(s)} = \frac{\omega_n^4}{s^4 + 2.1\omega_n s^3 + 3.4\omega_n^2 s^2 + 2.7\omega_n^3 s + \omega_n^4} \quad (19)$$

From equations (18 and 19.), we can determine the controller parameters as follows.

$$K_p^\theta = \frac{2.7\omega_n^3.\tau_{2\omega} - \omega_n^4.\tau_{2\omega}.K_p^\omega / K_i^\omega}{K_t K_j K_i^\omega} \quad (20)$$

$$K_i^\theta = \frac{\tau_{2\omega}.\omega_n^4}{K_t K_j K_i^\omega} \quad (21)$$

$$K_d^\theta = \frac{\left(2.1\omega_n.\tau_{2\omega} - \tau_{1\omega}\right)}{K_t K_j K_i^\omega} \quad (22)$$

3.2.2 Feed-forward Controller

According to block diagram shown in Fig. 3 with PI-D 2DOF controller, the closed loop transfer function with pre-filter and at $T_L(s) = 0$ is given by:

$$\frac{\theta_r(s)}{\theta_r^*(s)} = \frac{K_t K_j (K_p^\theta s + K_i^\theta).(K_p^\omega s + K_i^\omega)/\tau_{2\omega}}{s^4 + \tau_{3\theta}s^3 + \tau_{2\theta}s^2 + \tau_{1\theta}s + \hat{K}K_i^\theta}.G_{ff}(s) \quad 23)$$

Accordingly, we can obtain the feed forward controller transfer function that has the following relation from equations (19 and 23).

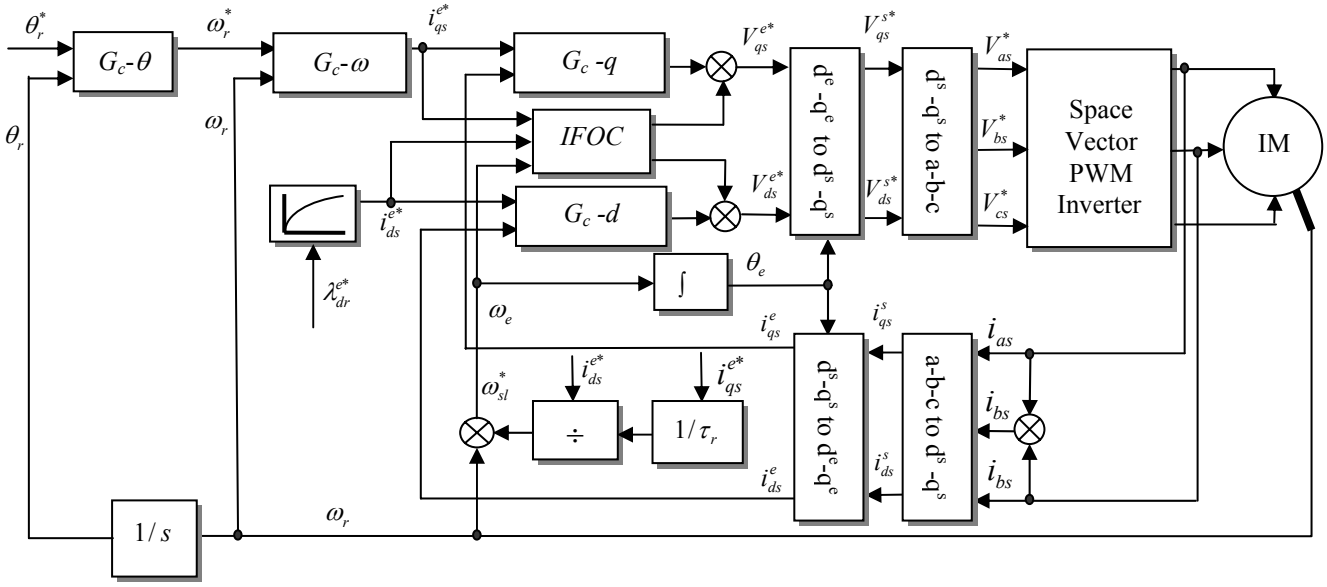

Fig. 1 Schematic block diagram of the IFOC induction machine drive system

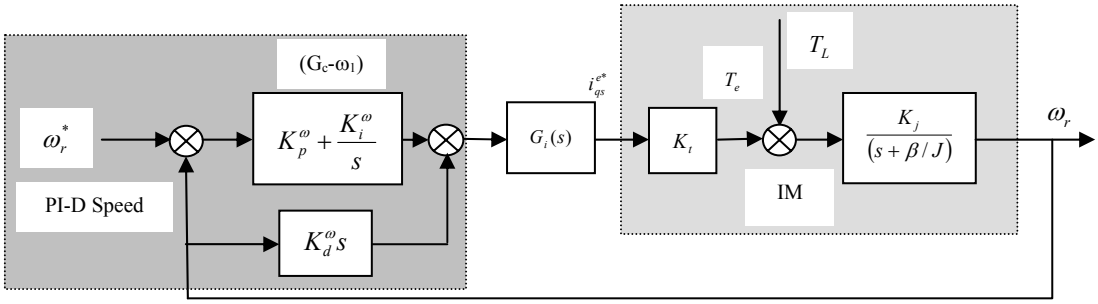

Fig. 2 Block diagram of induction machine speed control with PI-D controller

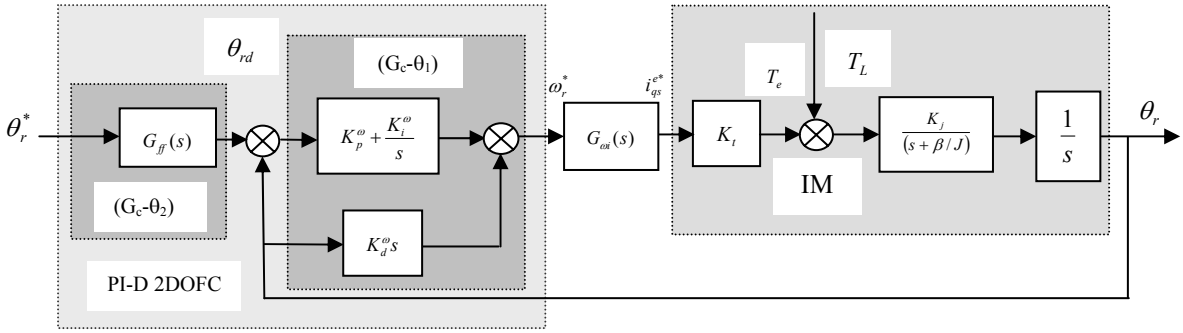

Fig. 3 Block diagram of induction machine position control with PI-D 2DOF controller

$$G_{ff}(s) = \frac{\omega_n^4.\tau_{2\omega}}{K_t K_j (K_p^\theta s + K_i^\theta).(K_p^\omega s + K_i^\omega)} \quad (24)$$

Equation (24) is a tow lag compensators but to speed up the response we add two zeros to obtain a lead-lag compensator. Therefore, the feed-forward compensator transfer function is given by:

$$G_{ff}(s) = \tilde{K}.\frac{(1+\tau_{lead}s)}{[1+(K_p^\theta / K_i^\theta)s]} \quad (25)$$

Where,

$$\tau_{lead} > (K_p^\theta / K_i^\theta),\ \tilde{K} = \omega_n^4 \tau_{2\omega} / K_t K_j K_i^\theta$$

$$\tau_{3\theta} = (\tau_{1\omega} + K_t K_j K_d^\theta)/\tau_{2\omega},\ \hat{K} = K_t K_j K_i^\omega / \tau_{2\omega}$$
$$\tau_{2\theta} = (K K_i^\omega + K_t K_j K_i^\omega K_d^\theta + K_t K_j K_p^\omega K_p^\theta)/\tau_{2\omega}$$
$$\tau_{1\theta} = (K_t K_j K_p^\omega K_d^\theta + K_t K_j K_i^\omega K_p^\theta)/\tau_{2\omega}$$

4 On-Line Trained Simple Neuro-Controller (SNC)

In this section, a proposed simple neuro-controller (SNC) with learning ability on-line and simple structure is described. Its training is on-line based on a modified error function that depends on the

input variable and the output variable and its derivative. The modified error function is used to improve the performance of the SNC which is trained on-line by the back propagation algorithm [10 - 11].

4.1 Back Propagation Algorithm with a Modified Error Function

The neural network needs to be trained to generate multiple input-output matching pattern. The training of the neural network is basically a process of finding the local minimum of a predefined objective function. The most popular training algorithm is the Bake Propagation (BP). The training can be off-line, on-line or combination of both. The input and output of a neuron j are given by the following equations.

$$S_{pj} = \sum_i W_{ji} O_{pi} + \phi_j \tag{26}$$

$$O_{pj} = F(S_{pj}) \tag{27}$$

The BP training algorithm is an iterative gradient algorithm designed to minimize the mean square error between the actual output of a feed forward net and the desired output. This technique uses a recursive algorithm starting at the output units and working back to the hidden layer to adjust the neural weights according to the following equations:

$$W_{ji}(t+1) = W_{ji}(t) + \Delta W_{ji}(t) \tag{28}$$

$$\Delta W_{ji}(t) = \varepsilon \delta_{pj} O_{pj} \tag{29}$$

$$\delta_{pj} = -\frac{\partial E_p}{\partial O_{pj}} . \bar{F}(S_{pj}) \tag{30}$$

The error function normally used in the standard BP algorithm is given by:

$$E_p = \frac{1}{2} \sum_j (t_{pj} - O_{pj})^2 \tag{31}$$

When neuron j is an output layer,

$$\frac{\partial E_p}{\partial O_{pj}} = (t_{pj} - O_{pj}) \tag{32}$$

When j is in hidden layer,

$$\frac{\partial E_p}{\partial O_{pj}} = \sum \delta_{pk} W_{kj} \tag{33}$$

The traditional error function is given in equation (32). The modified error function is based on the traditional error function, the error between the input and output variables, and the change of the controlled output. Therefore, equation (32) can be modified to the following equation to provide the modified error function (*mef*).

$$\frac{\partial E_p}{\partial O_{pj}} = \left[(t_{pj} - O_{pj}) - \frac{dO_{pj}}{dt} \right] \tag{34}$$

Where:

S_{pj} : input of neuron j for pattern p
O_{pj} : output of neuron j for pattern p
W_{ij} : weight from unit i to unit j
t_{pj} : target input
E_p : error function for pattern p
ε : learning rate
F : sigmoid activation function
t : time
δ_{pj} : error term for unit j
ϕ_j : bias

4.2 Simple Neuro-Controller (SNC)

The SNC consists of only one weight and one neuron with a linear hard limit activation function as shown in Fig. 4. The SNC output can be derived from Fig. 4 as follows:

$$u = xW - \phi \tag{35}$$

Based on the BP algorithm, the bias and weight change are:

$$\Delta W = \varepsilon . mef . x \tag{36}$$

$$\Delta \phi = -\varepsilon . mef \tag{37}$$

4.3 The Proposed Modified Error Function

The proposed modified error function *(mef)* is obtained by adding a term (*kdy/dt*) opposite to the traditional error (*x-y*) to change the overall error of the system and then speed up the system output response to its target. Also, the *mef* is used to modify the weight *W* and bias θ on-line as given by equations (35-38) and as shown in Fig. 4.

$$mef = \left[(x - y) - k \frac{dy}{dt} \right] \tag{38}$$

Where:

u : the controller output
y : the controlled variable
x : reference input
k : constant
mef : the modified error function, *f(x, y, ky')*

Based on equations (35-38), the SNC weight update depends on two parameters named *k* and ε. For each controller these two parameters are selected by trial and error based on the author experiences.

4.4 Training Process

The SNC is trained on-line directly from the system inputs and outputs. There is no need to determine the states of the system and reference model or parameters identification. From the inputs and outputs of the system, the *mef* computes the error

which is back propagated the SNC to update its weights and then the SNC outputs is calculated.

5 Design of the On-Line Trained Simple Neuro-Controllers (SNCs)

This section provides the design of a four SNCs, d-q axes stator current controllers speed controller and position controller.

5.1 Design of SNC Current Controllers

5.1.1 Q-axis SNC Current Controller (G_c-q)

The proposed SNC-q controller has i_{qs}^{e*} as the controller input, and i_{qs}^{e} as the controlled variable. The *mef* of the SNC-q current controller is given by equation (34). Using this function along with equations (36-37), the controller output can be calculated as given in equation (35).

$$mef_q(t) = e_q(t) - k_q \frac{d}{dt} i_{qs}^{e} \tag{39}$$

$$e_q(t) = \left(i_{qs}^{e*}(t) - i_{qs}^{e}(t)\right) \tag{40}$$

5.1.2 D-axis SNC Current Controller (G_c-d)

Similarly, the *mef* of SNC-d current controller is given by equation (41). The controller output can be calculated from the weight , bias and the *mef* given by equation (41), the controller output can be calculated.

$$mef_d(t) = e_d(t) - k_d \frac{d}{dt} i_{ds}^{e} \tag{41}$$

$$e_d(t) = \left(i_{ds}^{e*}(t) - i_{ds}^{e}(t)\right) \tag{42}$$

5.2 Design of SNC Speed Controller (G_c-ω)

Similar to the current controllers, the proposed SNC speed controller has ω_r^*, ω_r as the controller input and the controlled variable respectively. The *mef* of the SNC-**ω** speed controller is given by the following equation.

$$mef_\omega(t) = e_\omega(t) - k_\omega \frac{d}{dt} \omega_r \tag{43}$$

$$e_\omega(t) = \left(\omega_r^*(t) - \omega_r(t)\right) \tag{44}$$

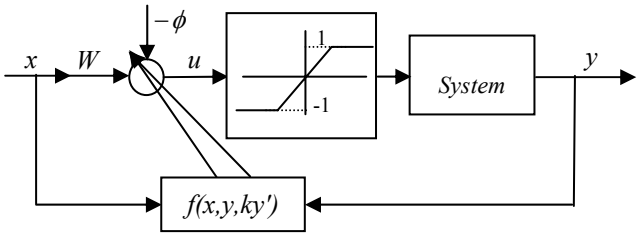

Fig. 4. Single neuron configuration

5.3 Design of SNC Position Controller (G_c-θ)

Also, the proposed SNNC-**θ** controller has θ_r^*, θ_r as the controller input and the controlled variable respectively. The SNNC-**θ** error function is given by the following equation:

$$mef_\theta(t) = e_\theta(t) - k_\theta \frac{d}{dt} \theta_r \tag{45}$$

$$e_\theta(t) = \left(\theta_r^*(t) - \theta_r(t)\right) \tag{46}$$

6 Simulation Results of the Drive System

The simulation of the proposed control scheme for IFOC induction machine drive system has been carried out using PCMATLAB package. The dynamic performance of the drive system for different operating conditions has been studied with the application of the four SNCs to the d-q currents, speed and position loops and then compared with the conventional controllers. Taking into consideration the parameter variations of the induction machine, the drive system performance has been tested under load changes and set-point variations.

6.1 Dynamic Performance Under Different Loads

The dynamic performance of the drive system under the disturbances of step change in reference position and step change in load is shown in Figures (5-6). Fig. 5 illustrates the dynamic response of the drive system with the application of SNCs and the dynamic response of the drive system with the conventional PI-D 2DOF position controller at the same conditions is illustrated in Fig. 6. Figures (5-6) show the position tracking, speed response, current response, and load regulation performance under nominal parameters. At t=1.5 sec, an external load of 10 N.m is applied to the drive system for both controllers. It is obvious that the proposed SNCs provide a rapid and accurate response for the reference within 0.55 sec. Also, the SNCs quickly return the position to the command position within 0.55 sec under full load with a maximum dip of 0.01 radian. While the position response of the conventional control scheme provides a slow response for the reference of about 1 second and has a long recovery time of 1 second and large dipping in position of about 0.43 radian under load changes as shown in Fig. 6. Fig. 7 proves that IFOC is achieved during load changes ($\lambda_{dr}^{e} = \lambda_r^{e*}$ and $\lambda_{qr}^{e} = 0$). Also, this figure illustrates that the proposed SNCs

control scheme provides robust performance than the conventional PI-D 2DOF controller. The dynamic performance introduced through Figures (5-7) reveals that the proposed SNCs control scheme has an extremely quick position response and is influenced slightly by the load disturbance.

6.2 Influences of Parameter Variations

The position response and the load regulation performance of the proposed SNCs and the conventional controller are shown in Figures (8-9) respectively under parameter variation of the machine. It can be seen that from these figures that the drive system with SNCs controllers is insignificantly affected by variations in the induction machine parameters while the drive system response with the PI-D 2DOF controller shows a significant effect of the parameter variations.

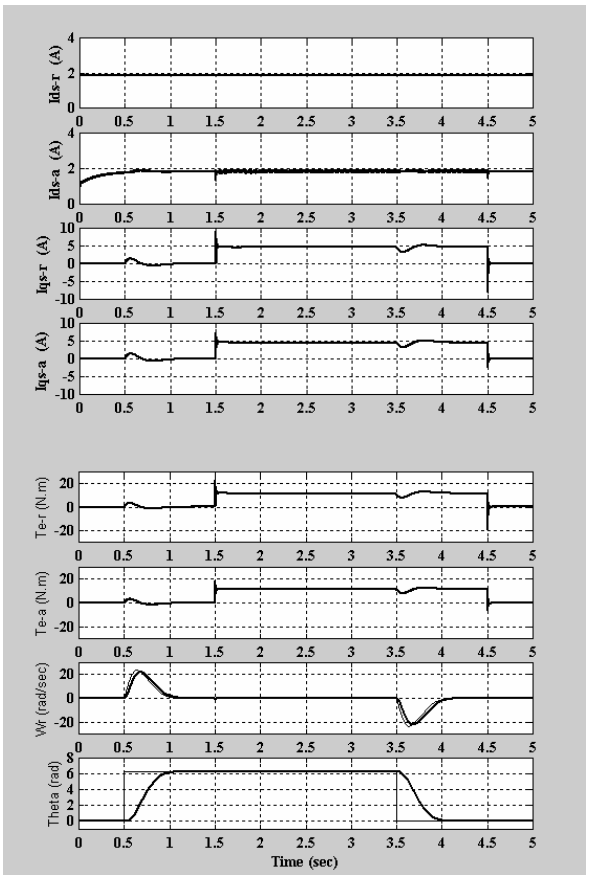

Fig. 5. Dynamic performance of the current, speed and position with the proposed SNCs controllers

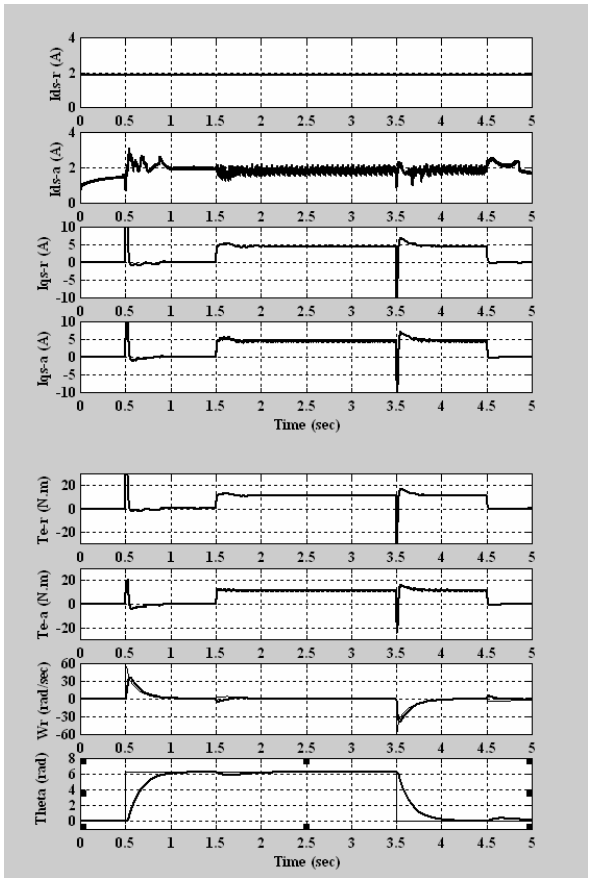

Fig. 6. Dynamic performance of the current, speed and position with the proposed PI-D 2DOF position controller

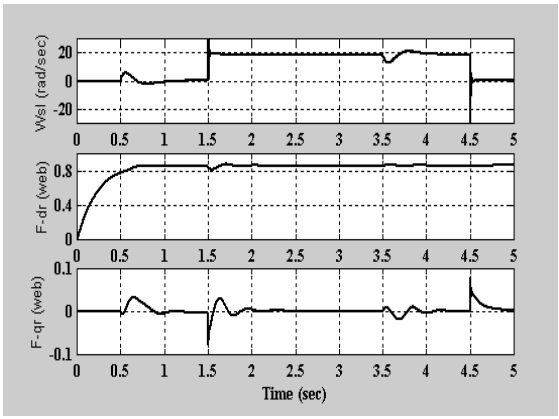

Fig. 7-a. Performance of the IFOC variables, ω_{sl}, λ^{e}_{dr}, λ^{e}_{qr}, with SNCs controllers

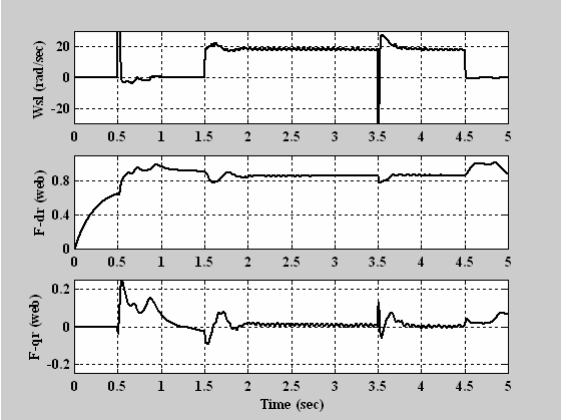

Fig. 7-b. Performance of the IFOC variables, ω_{sl}, λ_{dr}^{e}, λ_{qr}^{e}, with PI-D 2DOF position controller

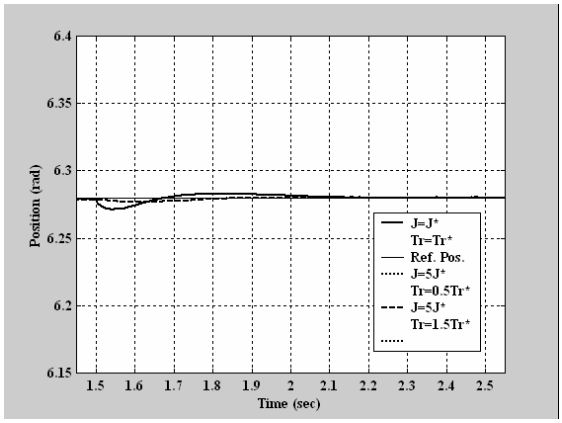

Fig. 8-a. Load regulation performance under parameter variations with the proposed SNCs controllers

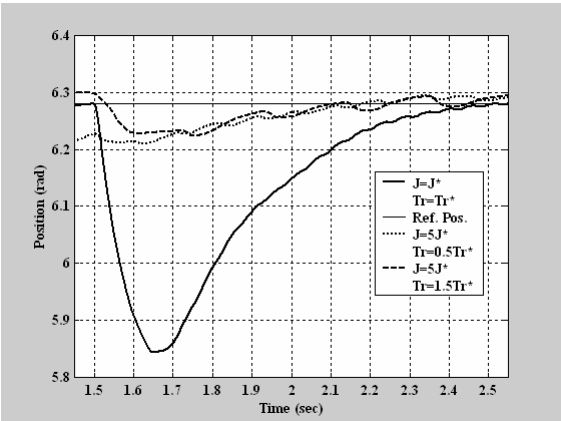

Fig. 8-b. Load regulation performance under parameter variations with the proposed PI-D 2DOF position controller

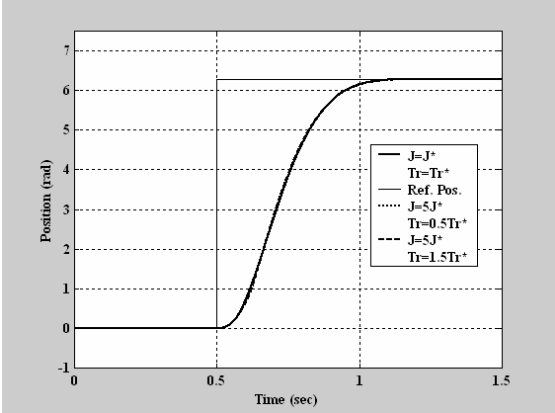

Fig. 9-a. Step response performance under parameter variations with the proposed SNCs controllers

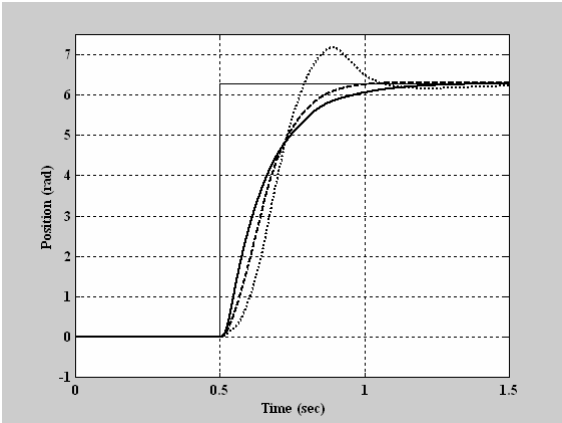

Fig. 9-b. Step response performance under parameter variations with the proposed PI-D 2DOF position controller

7 Conclusion

In this paper, a SNC control system design for IFOC of induction machine drive system has been presented. The SNC control constitute a simple structure that is applied to the induction machine drive system. In spite of the simple structure of SNCs, the obtained results show that those controllers can provide a fast and accurate dynamic response in tracking and disturbance rejection characteristics under parameter variations. At the same time, a reduction of the computation time has been occurred as a result of the simple construction of the four SNCs. The proposed SNC controller can compensate the induction machine drive system at nominal values and is insignificantly affected by variations in the induction machine's parameters. The position response of this proposed SNC control scheme was influenced slightly by the load disturbance, whether the system parameters varied

or not. However, the position response of the conventional control scheme did have a long recovery time. Simulation results demonstrate that the proposed SNC control scheme has a robust position response and can rapidly cancel a load disturbance and its superiority compared with the PI-D 2DOFC position controller for IFOC induction machine drive system.

8 Appendix

Table 1 shows the machine parameters measured by means of no-load and locked rotor tests.

Type: 3-phase induction motor, Y-connection, 1.5 kW, 4-poles, 380 V/3.8 A, 50 Hz
$R_s = 6.29\,\Omega, R_r = 3.59\,\Omega$,
$L_s = L_r = 480\,mH, L_m = 464\,mH$,
$J = 0.038\,\text{kg.m}^2$, $\beta = 0.008345$ N.m/rad/sec

Table 1 Machine parameters

References:

[1] Fayez F. M. El-Sousy, Faeka M.H. Khater and Farouk I. Ahmed, Analysis and Design of Indirect Field Orientation Control for Induction Machine Drive System, *Proceeding of the 38th SICE annual conference, SICE99*, Iwate, Japan, July 28-30, 1999, pp. 901-908.

[2] Fayez F. M. El-Sousy, Design and Implementation of 2DOF I-PD Controller for Indirect Field Orientation Control Induction Machine Drive System, *ISIE 2001 IEEE International Symposium on Industrial Electronics, Pusan, Korea*, June 12-16, 2001, pp. 1112-1118.

[3] Fayez F. M. El-Sousy and Maged N. F. Nashed, Robust Fuzzy Logic Current and Speed Controllers for Field-Oriented Induction Motor Drive, *The Korean Institute of Power Electronics (KIPE), Journal of Power Electronics (JPE)*, April 2003, Vol. 3, No. 2, 2003, pp. 115-123,.

[4] El-Sharkawy, M. A., Neural network application to high performance electric drive system, *Proceeding of ICEON'95*, 6-10 November 1995, USA, pp. 44-49.

[5] Karlik B. and Gulez, K., The performance analysis of induction motor with artificial neural networks, *Proceeding of ICEON'95*, 6-10 November 1995, USA, pp. 1452-1455.

[6] Ba-Razzouk, A. et al, Field-oriented control of induction motors using neural network decouplers, *Proceeding of ICEON'95*, 6-10 November 1995, USA, pp. 1428-1433.

[7] Razzouk, A. and Cheriti, A., Field-oriented control of IM using neural-network decouplers, *IEEE Trans. PE*, Vol. 12, No. 4, July 1997, pp. 752-763.

[8] Tsong-Terng Sheu and Tien-Chi Chen, Self-tuning control of induction motor drive using neural network identifier, *IEEE Trans. Energy Conversion*, Vol. 14, No. 4, 1999, pp.

[9] Ahmed Rubaai and Kankam M., Adaptive tracking controller for induction motor drives using online training of neural networks, *IEEE Trans. Industrial Appl*. 2000, vol. 36, no. 5, pp.

[10] Fayez F. M. El-Sousy and Salem, M. M., Robust Neural Network Controllers for Indirect Field Orientation Control of Induction Machine Drive System, *The 2002 International Conference on Control and Automation (ICCA'02)*, June 16-19, , Xiamen, China, 2002.

[11] Salem, M. M., Zaki, A. M., Mahgoub, O. A. Abu El-Zahab, E. and Malik, O. P., Experimental Studies with a Simple Neuro-Controller Based Excitation Controller, *IEE Proceedings, Gen., Trans. and Distr.*, Vol. 149, No. 1, January 2002, pp.108-113.